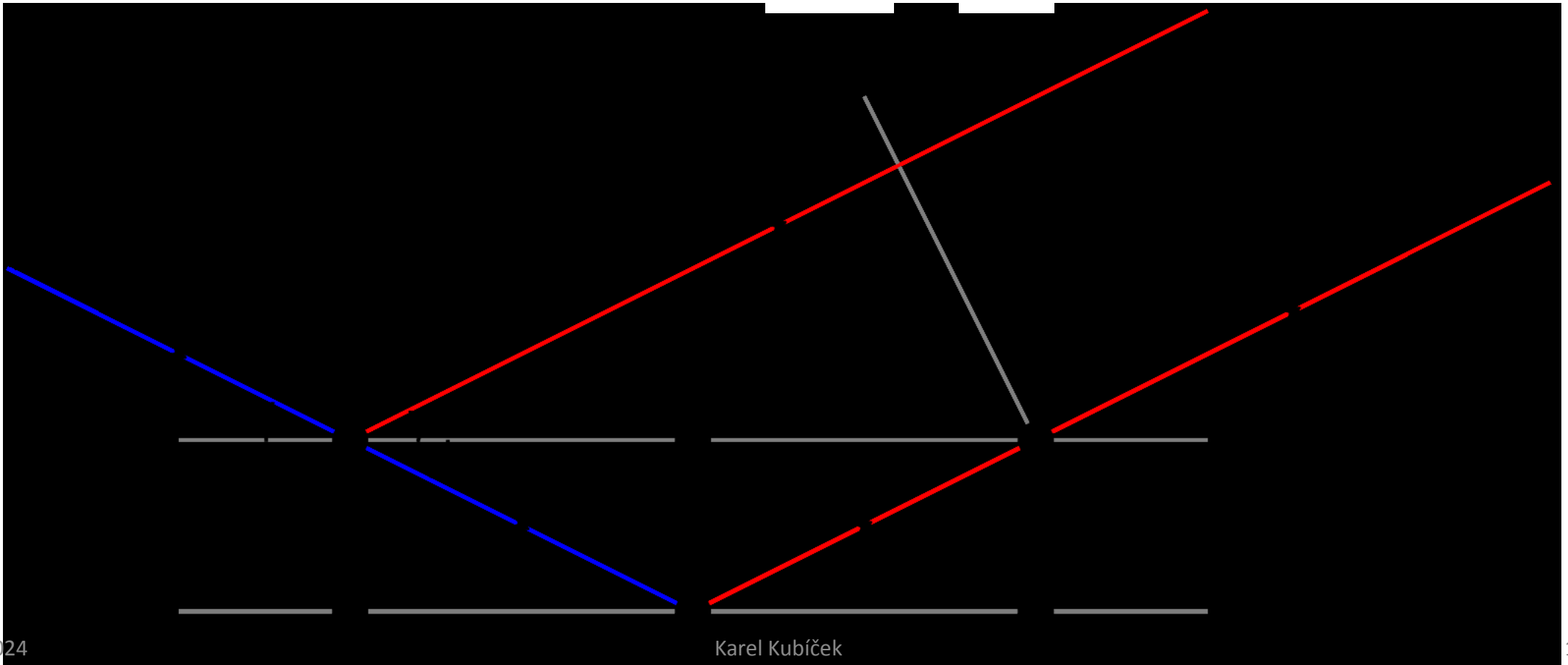


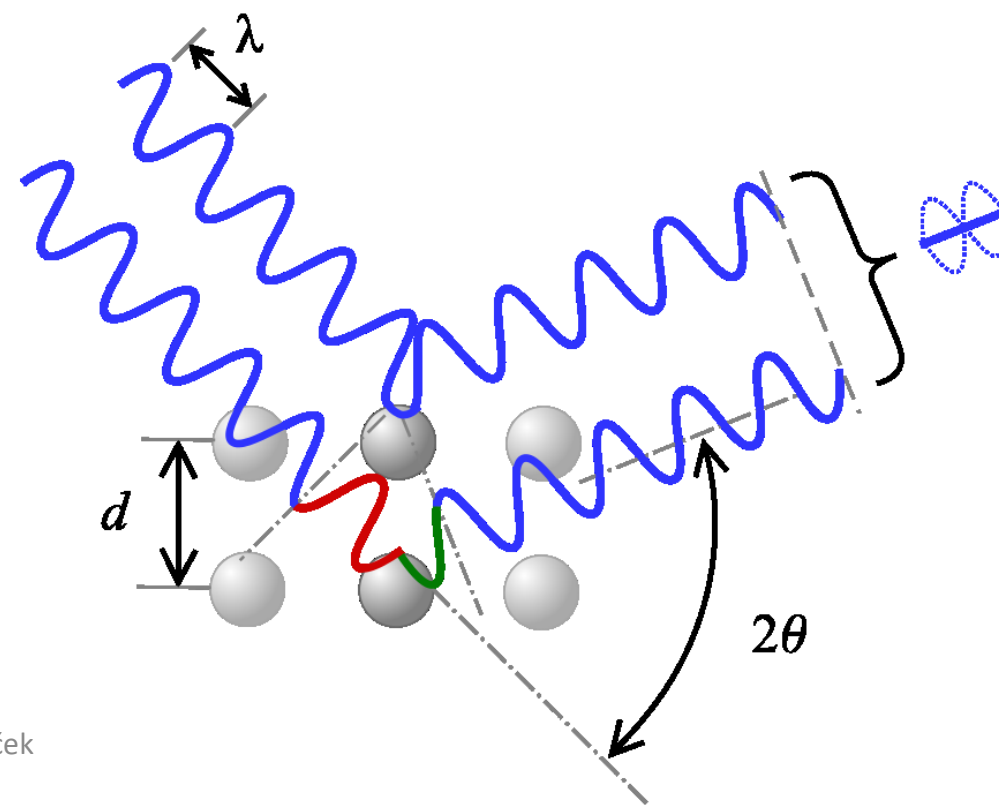
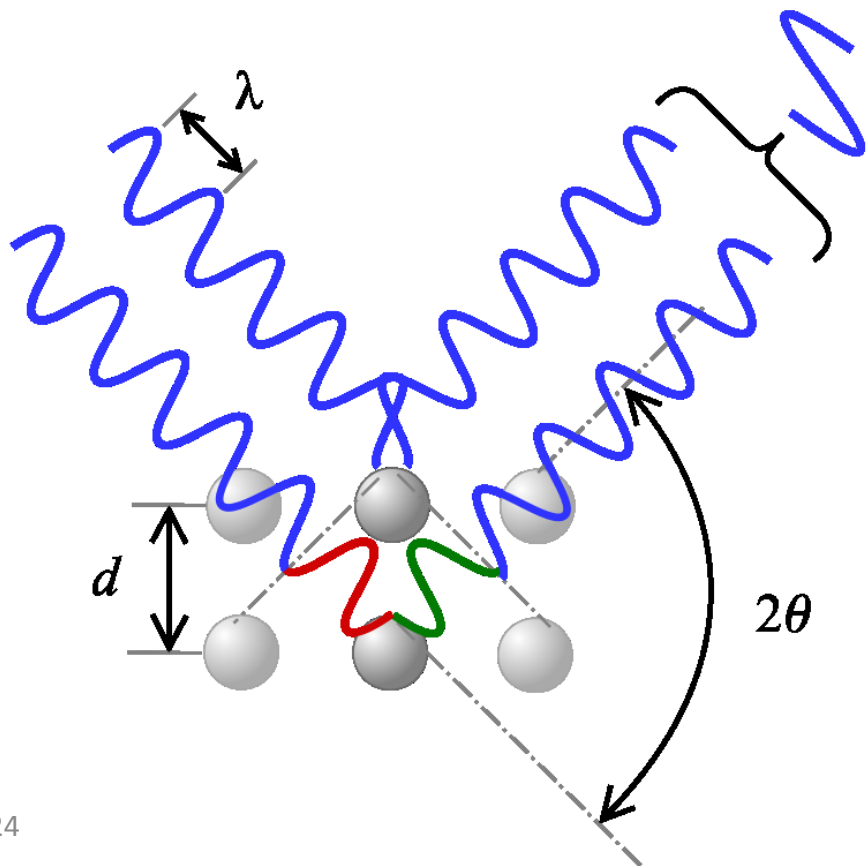
# Bragg's law

$$2d \sin\Theta = n\lambda$$

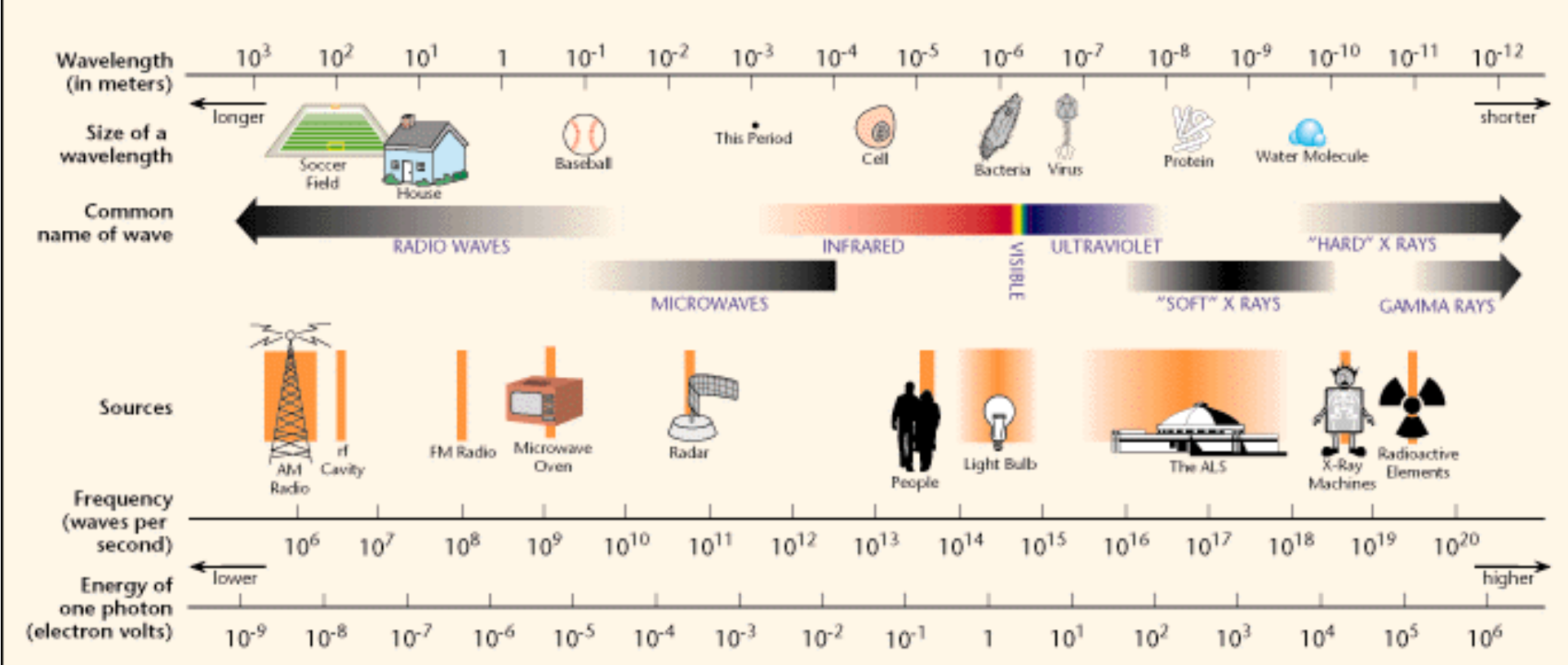


# Bragg's law

$$2d \sin\Theta = n\lambda$$

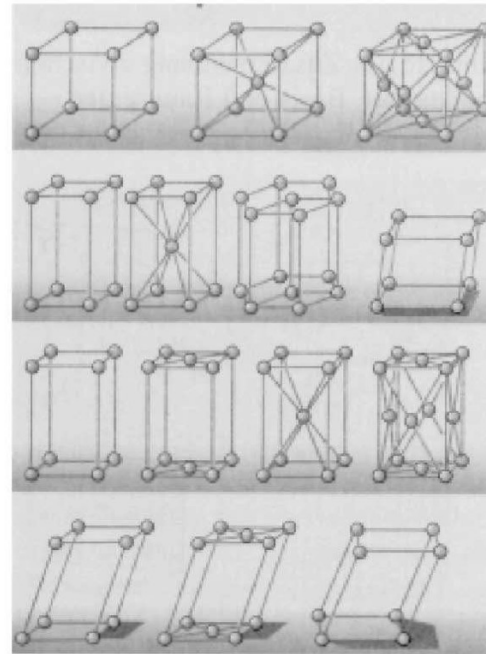
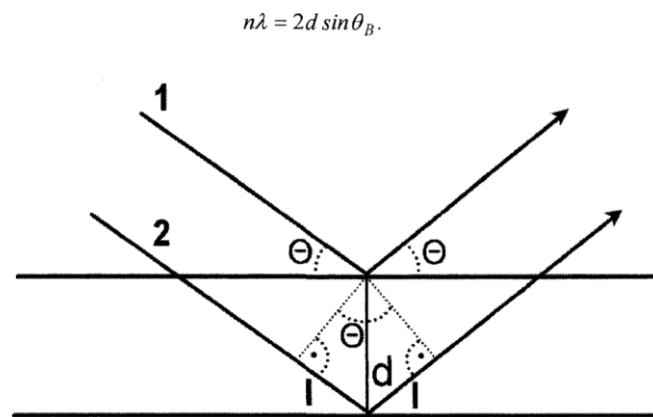


# THE ELECTROMAGNETIC SPECTRUM



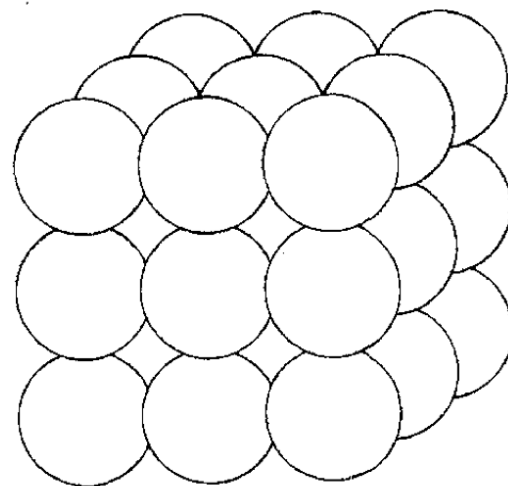
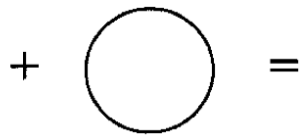
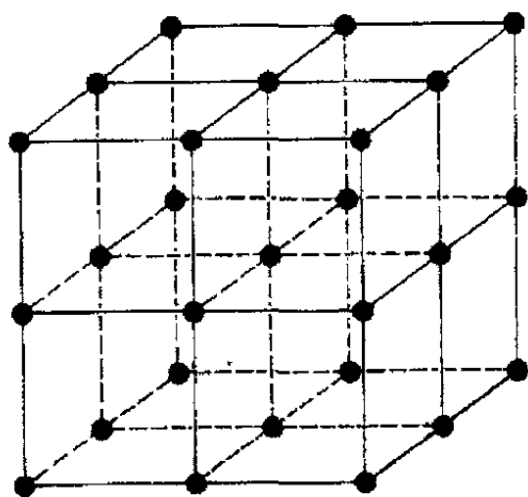
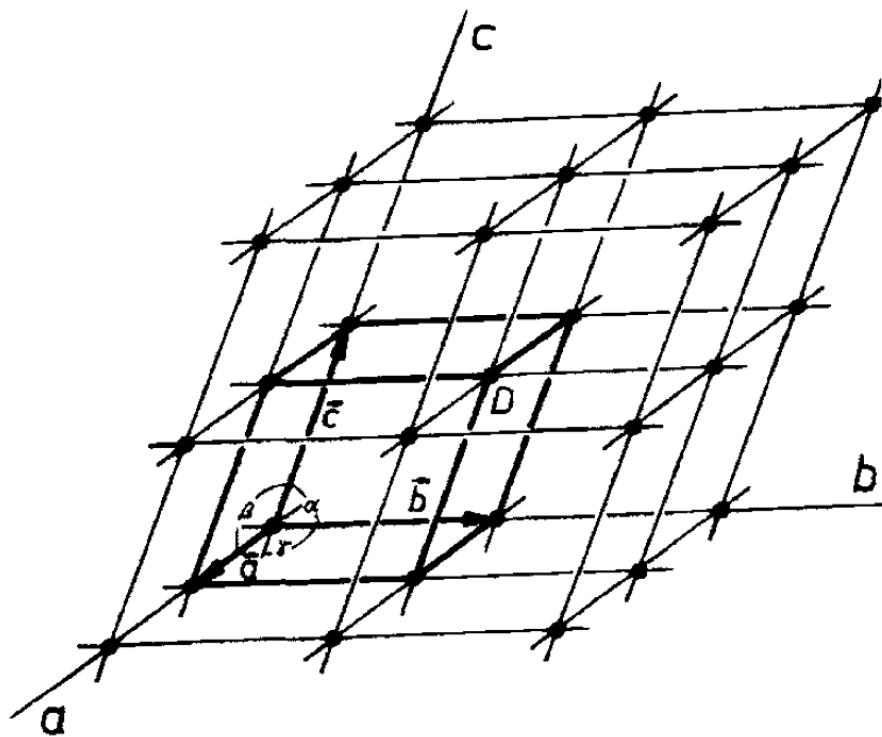
# Rentgenstrukturní analýza

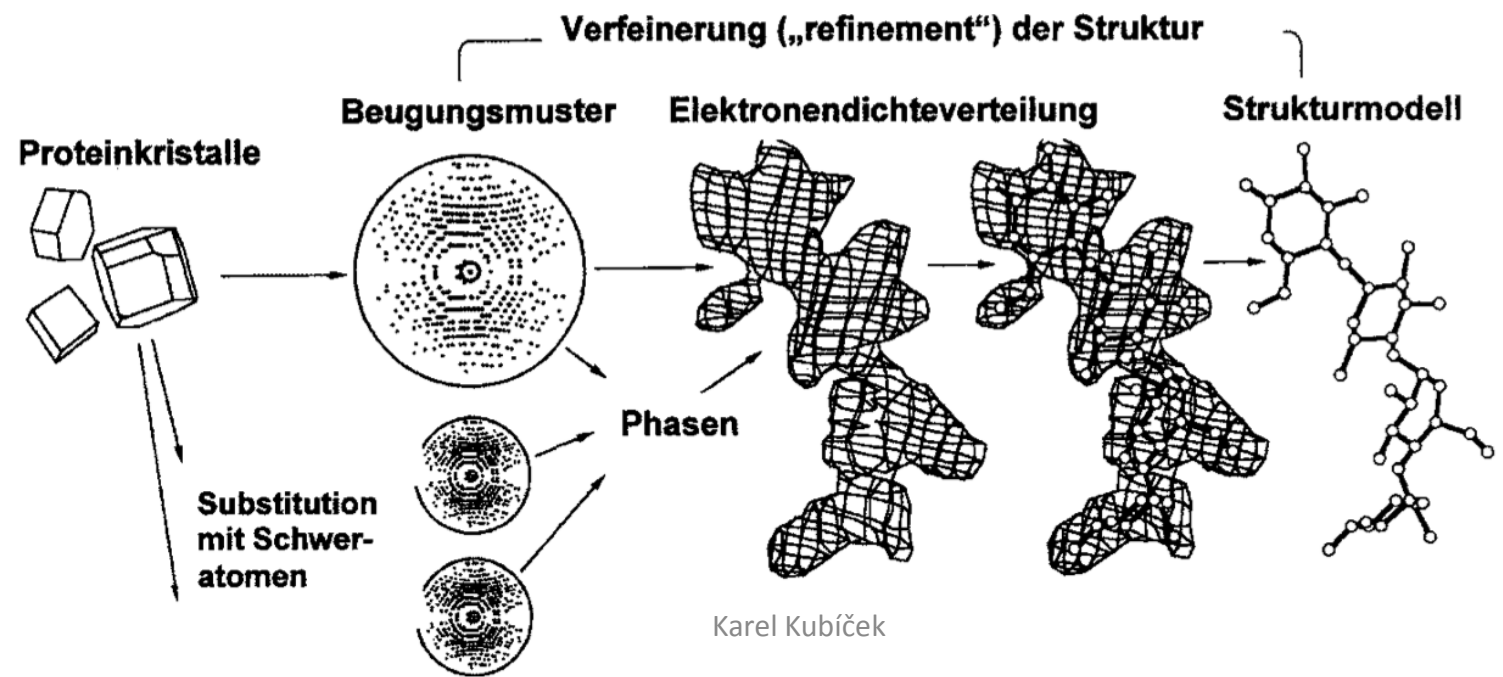
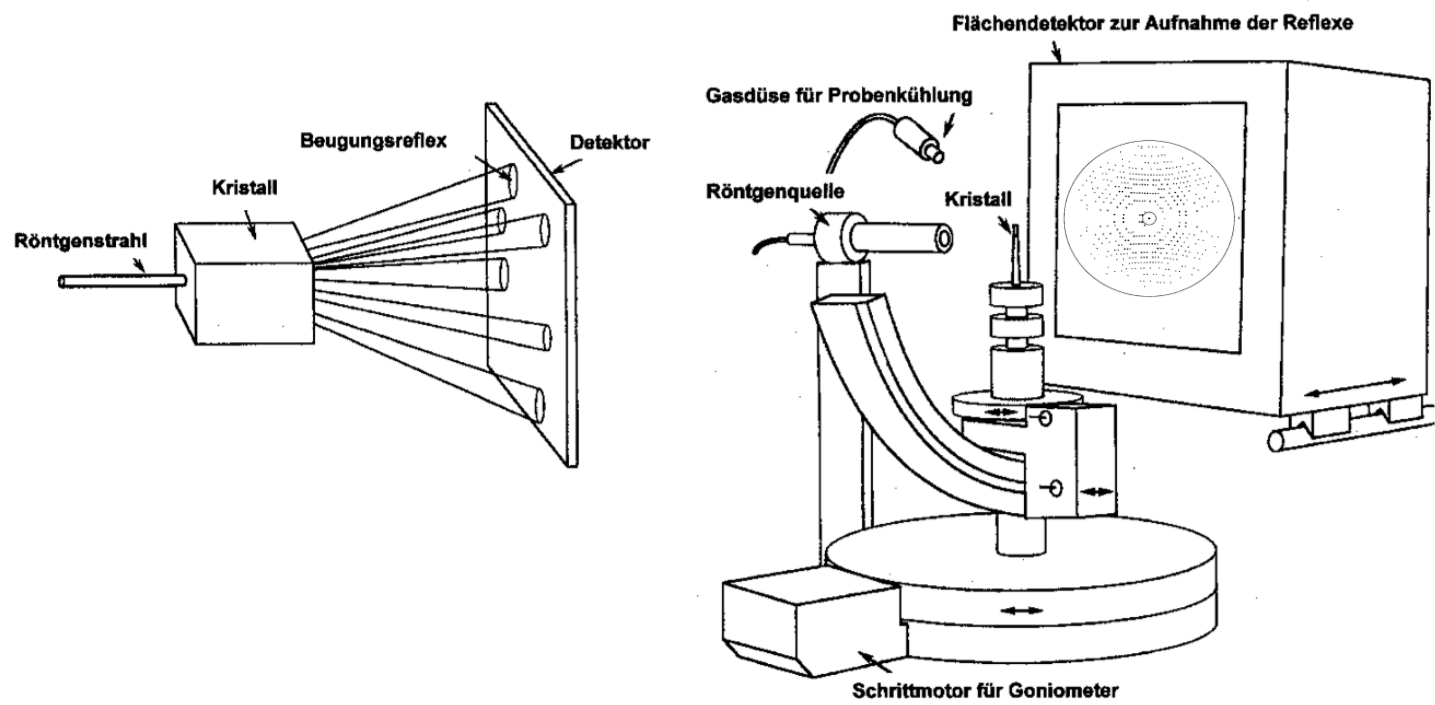
Krystalová mřížka působí na rentgenové záření jako optická mřížka na viditelné světlo. Nastávají ohybové jevy a na stínítku se objevuje difrakční obrazec. Tyto obrazce mohou být matematicky analyzovány, aby se získala informace o rozložení elektronů v molekulách tvořících krystal.



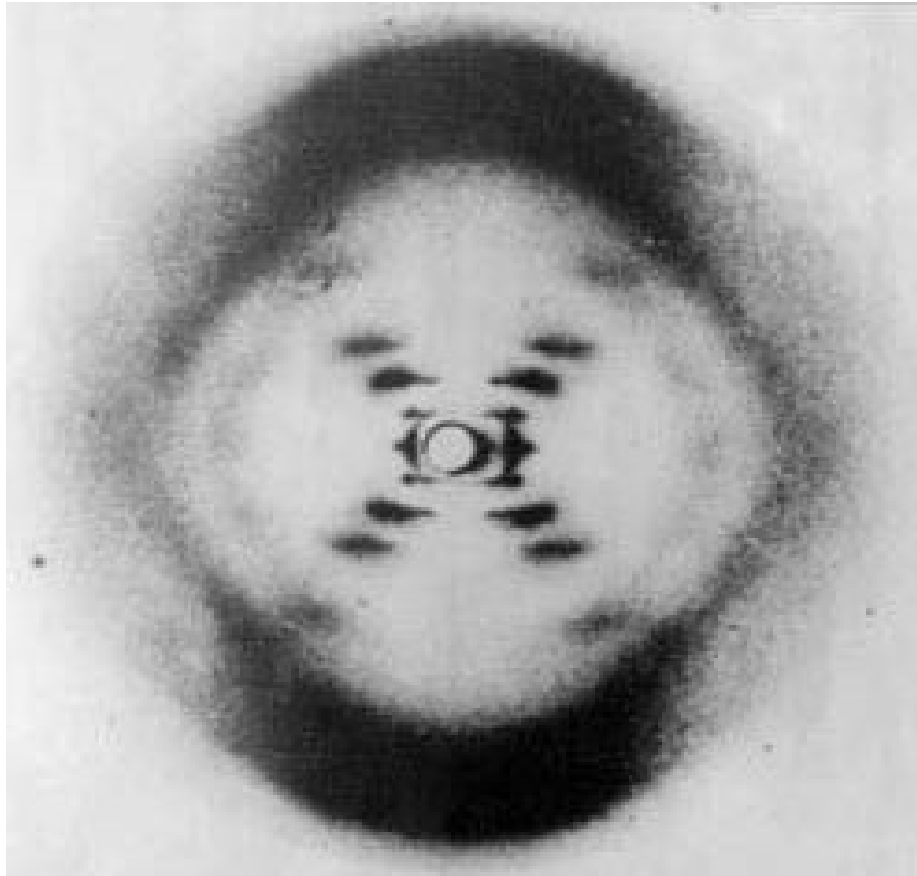
## Raumgitter

|   |                             |
|---|-----------------------------|
| $\alpha_1, \alpha_2, \alpha_3 \neq 90^\circ$ :                              | triklin                     |
| $\alpha_1 = \alpha_2 = 90^\circ$ ,<br>$\alpha_3 \neq 90^\circ$ :            | monoklin                    |
| $\alpha_1 = \alpha_2 = \alpha_3 = 90^\circ$ ,<br>$a_0 \neq b_0 \neq c_0$ :  | orthorhombisch              |
| $\alpha_2 = \alpha_3 = 90^\circ$ ,<br>$\alpha_1 = 60^\circ$ , $b_0 = c_0$ : | hexagonal                   |
| $\alpha_1 = \alpha_2 = \alpha_3 \neq 90^\circ$ ,<br>$a_0 = b_0 = c_0$ :     | trigonal<br>(rhomboedrisch) |
| $\alpha_1 = \alpha_2 = \alpha_3 = 90^\circ$ ,<br>$a_0 = b_0 \neq c_0$ :     | tetragonal                  |
| $\alpha_1 = \alpha_2 = \alpha_3 = 90^\circ$ ,<br>$a_0 = b_0 = c_0$ :        | kubisch                     |





Krystalogram **B-DNA** získaný v r. **1952** Rosalindou E. **Franklinovou**, na jehož základě **Watson** a **Crick** navrhli dvoušroubovicový model struktury DNA. **C. & W.** dostali v r. **1962** společně s Mauricem Hugh Frederick Wilkinsem NC za fyziologii a medicínu „za jejich objevy týkající se molekulární struktury nukleových kyselin a jejich významu při přenosu informací v živých organizmech“



F



C



W

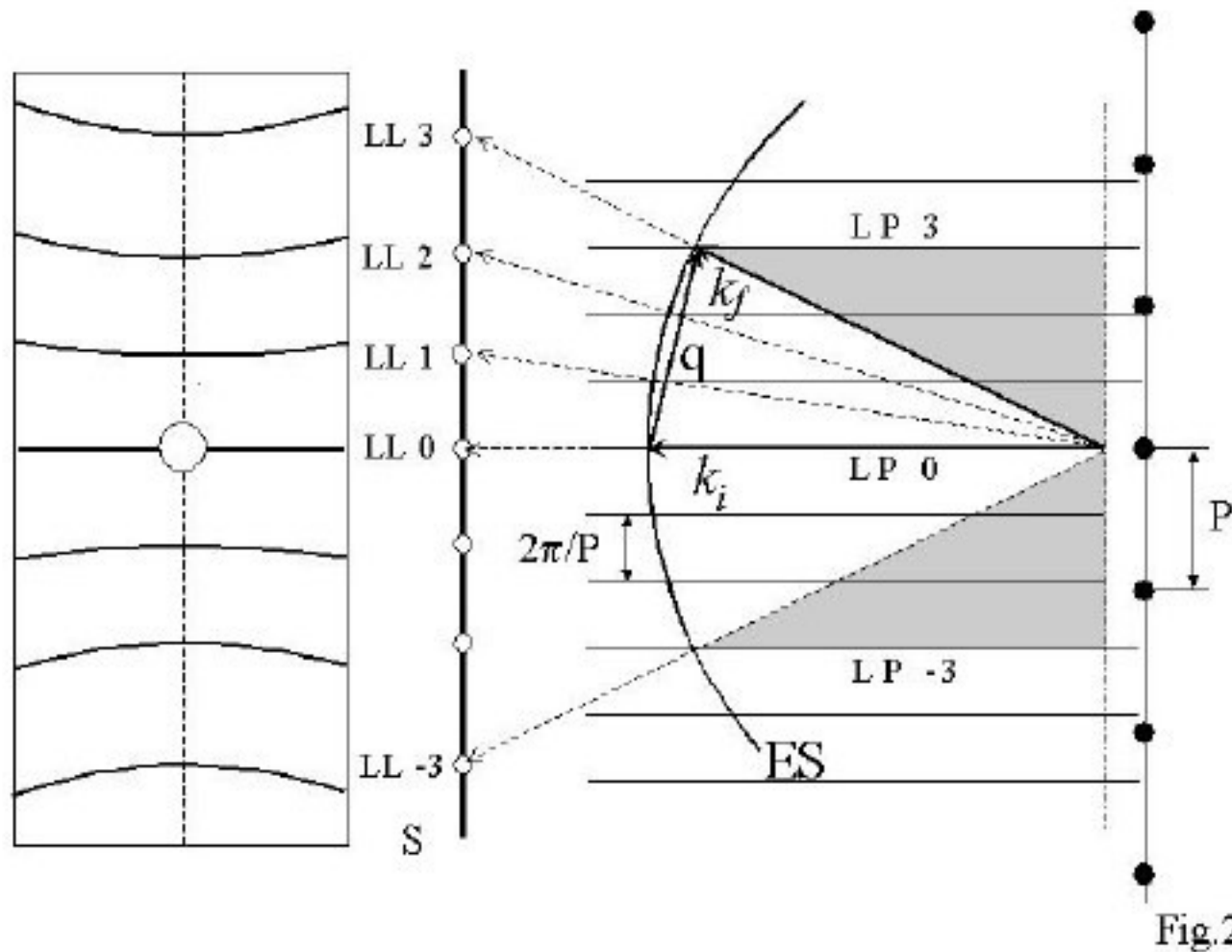
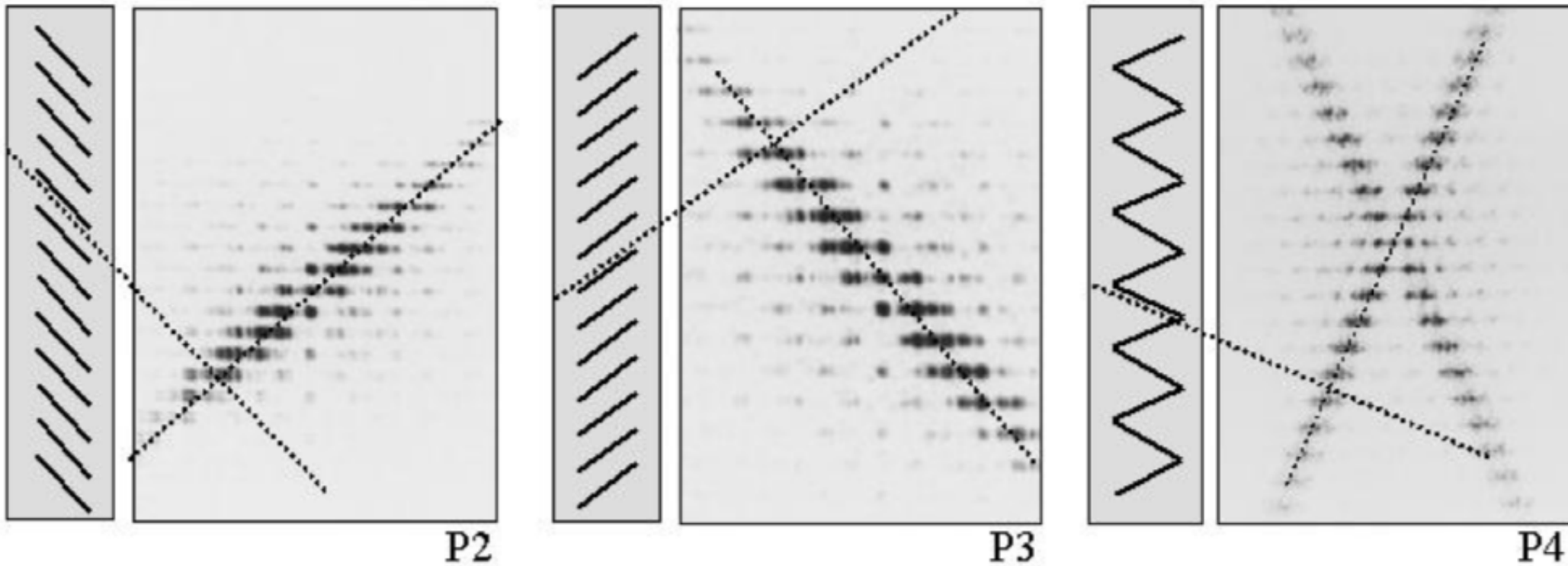


Fig.2

Fig.2 Principle of the geometrical construction of the hyperbolic layer lines in the X-ray diffraction pattern of a linear array of point scatterers (dark circles) with period  $P$ . ES: Ewald Sphere; LP: Layer Planes; S: observation Screen; LL: Layer Lines. The shaded regions are cones whose intersections by the screen generate the layer lines.

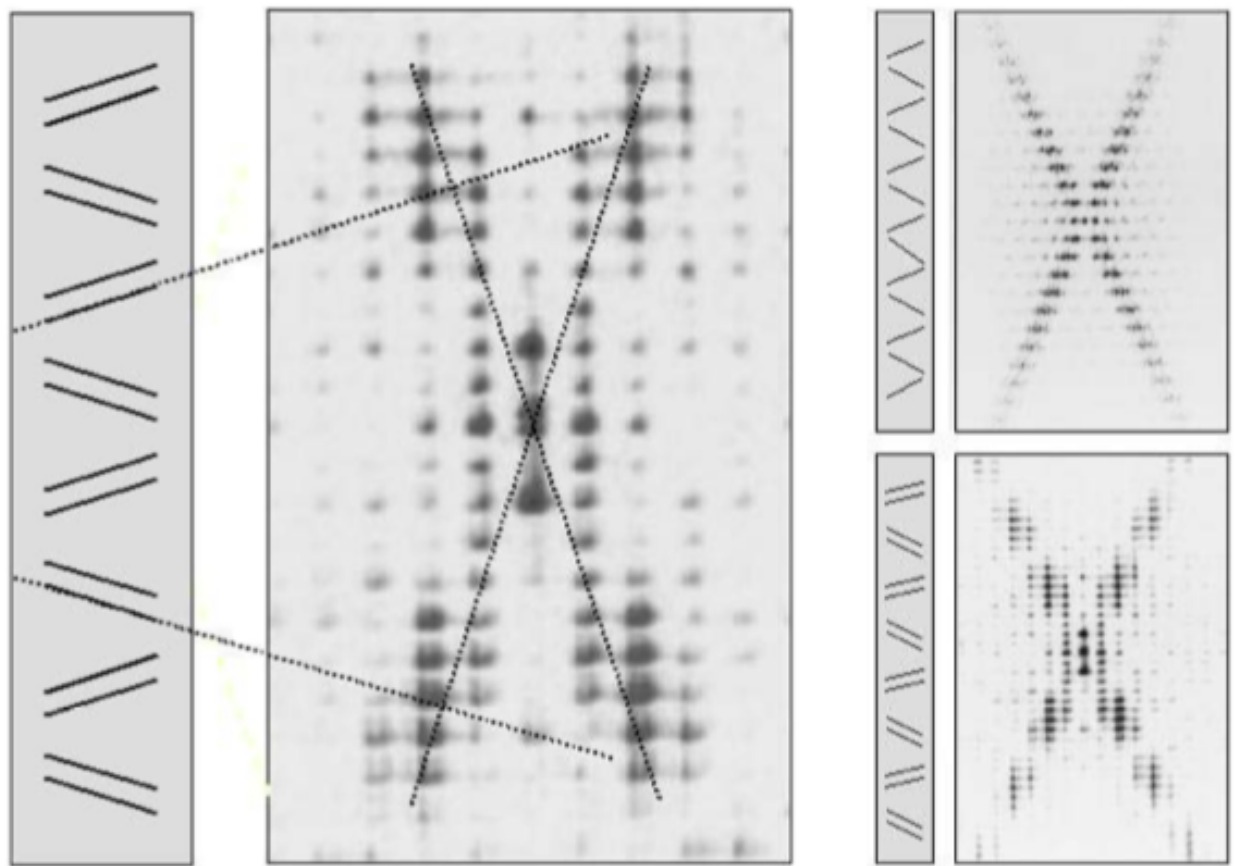




P2. A set of equidistant slits rotated clockwise diffracts light along regularly spaced layer lines. The band of maximal intensities is perpendicular to the slits (thin dotted lines).

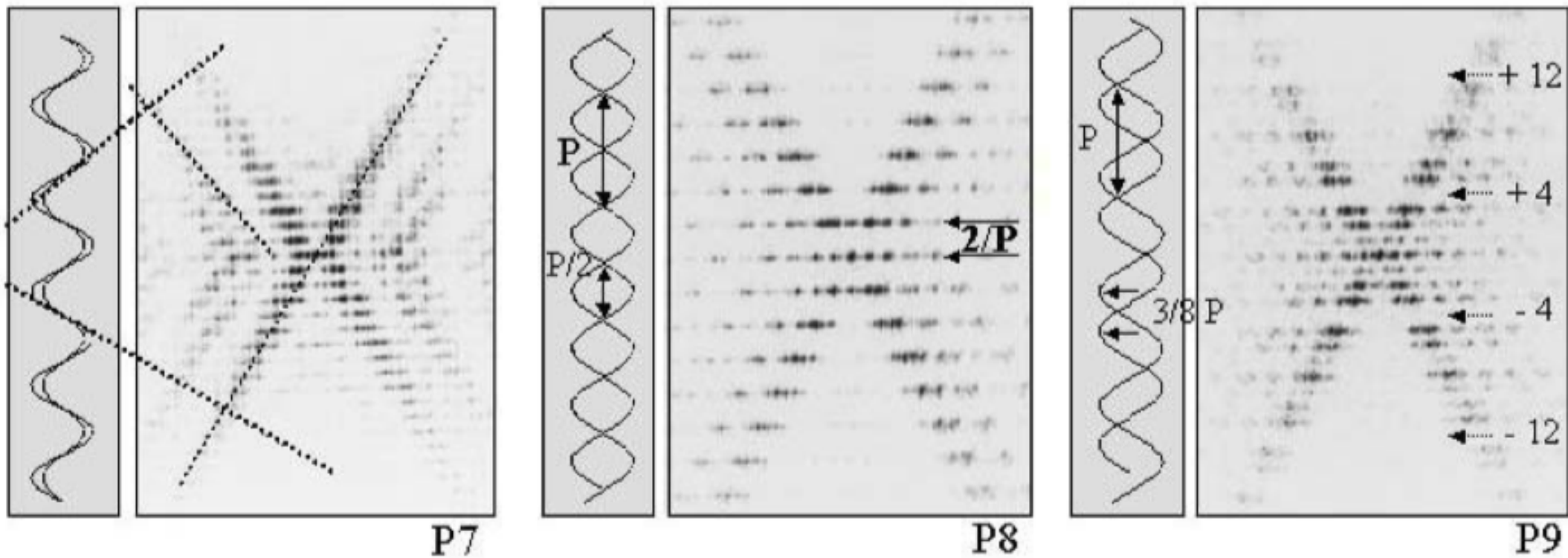
P3. A set of equidistant slits rotated anti clockwise diffracts light along regularly spaced layer lines. The band of maximal intensities is perpendicular to the slits (thin dotted lines).

P4. A zigzag motif diffracts light to form a Saint Andrew cross. The arms of the cross are perpendicular to the zigzagging slits (thin dotted lines).



P5

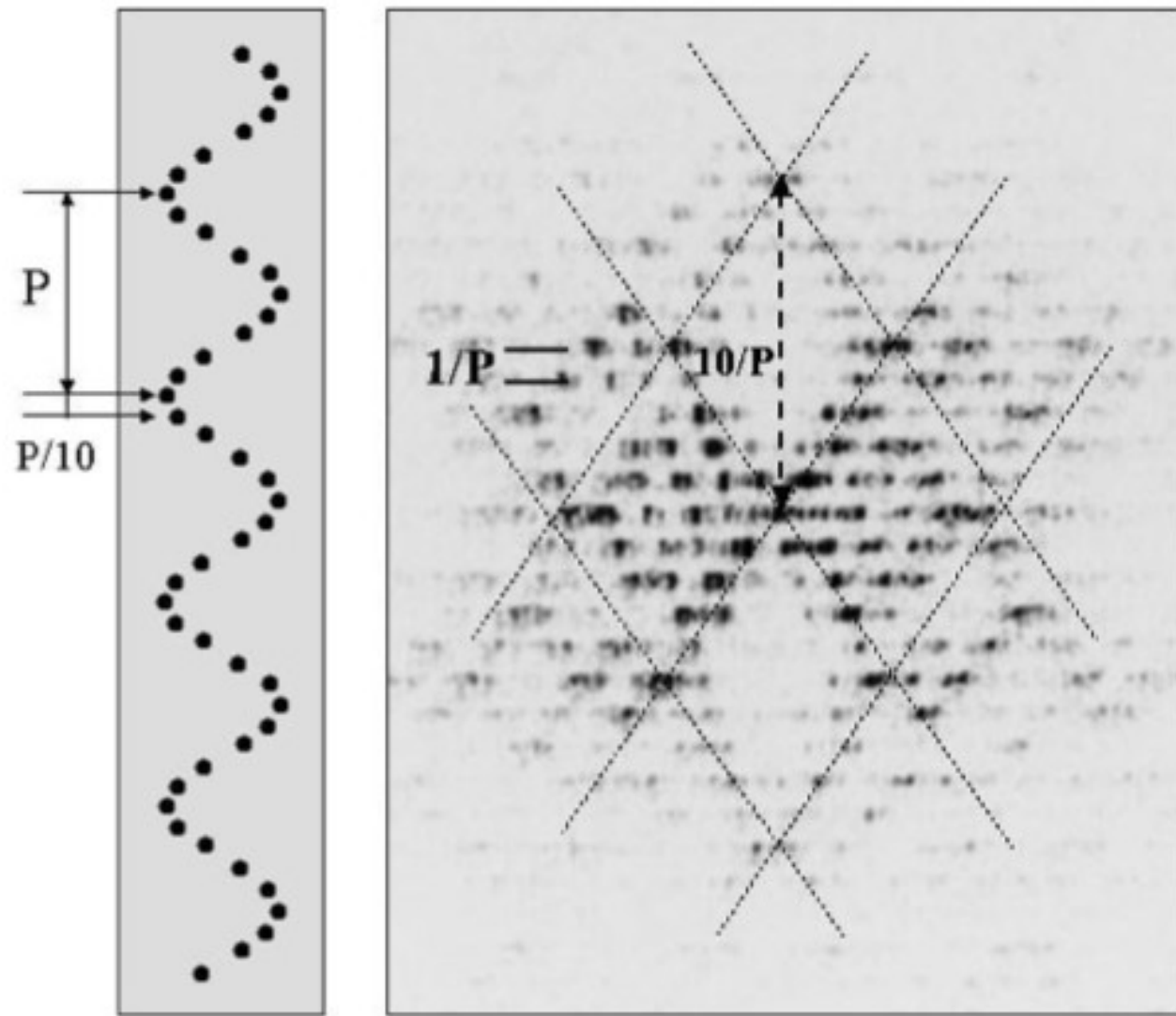
P5. A zigzag double slit motif diffracts light along regularly spaced layer lines. The motifs are arranged on a regular 2-D lattice on panel P5 of the slide, resulting in a spotty diffraction pattern. The maximal diffracted intensities define a Saint Andrew cross whose arms are perpendicular to the slits (thin dotted lines). The cross arms are clearly visible only at high- $l$  layer lines (see text). The two reduced patterns on the right reproduce P4 (upper right) and P5 (lower right) for comparison. Notice the modulation of the arms of the Saint Andrew cross of the double slit motif (lower right).



P7. Two coaxial sinusoidal motifs with different amplitudes. The intensities diffracted by the small sine wave fall within the east and west angles of the Saint Andrew cross of the large sine wave. There is no intensity diffracted in the meridian angles of the large sine wave cross.

P8. A motif with two out-of-phase sine waves. Note that the true period of the motif is half the sine wave period. The layer line spacing is doubled as compared to the spacing of a single sine wave.

P9. A motif with two sine waves separated by  $3P/8$ . Note the extinction of the 4<sup>th</sup> layer lines.



P10

P10. Diffraction by an atomic sinusoidal motif. Note the diamond pattern (dotted lines) and the absence of intensity in the meridian diamonds.

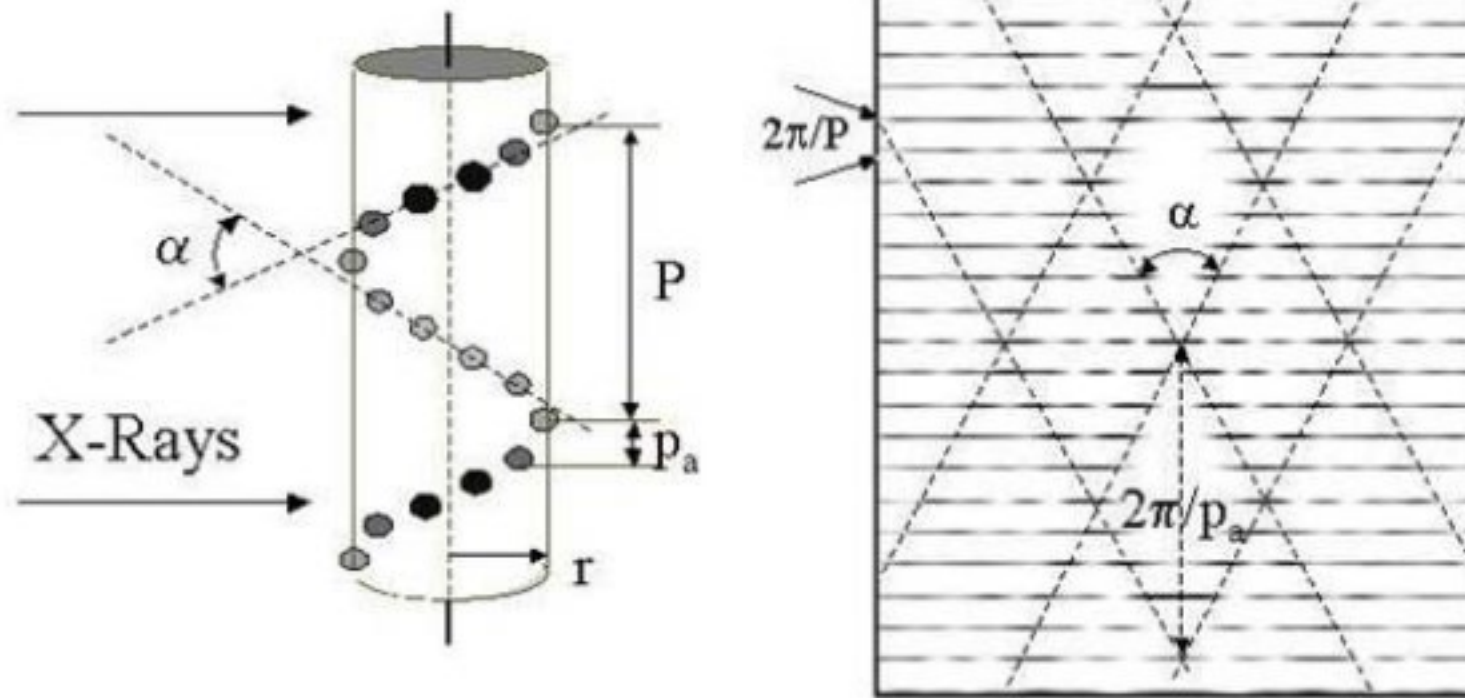
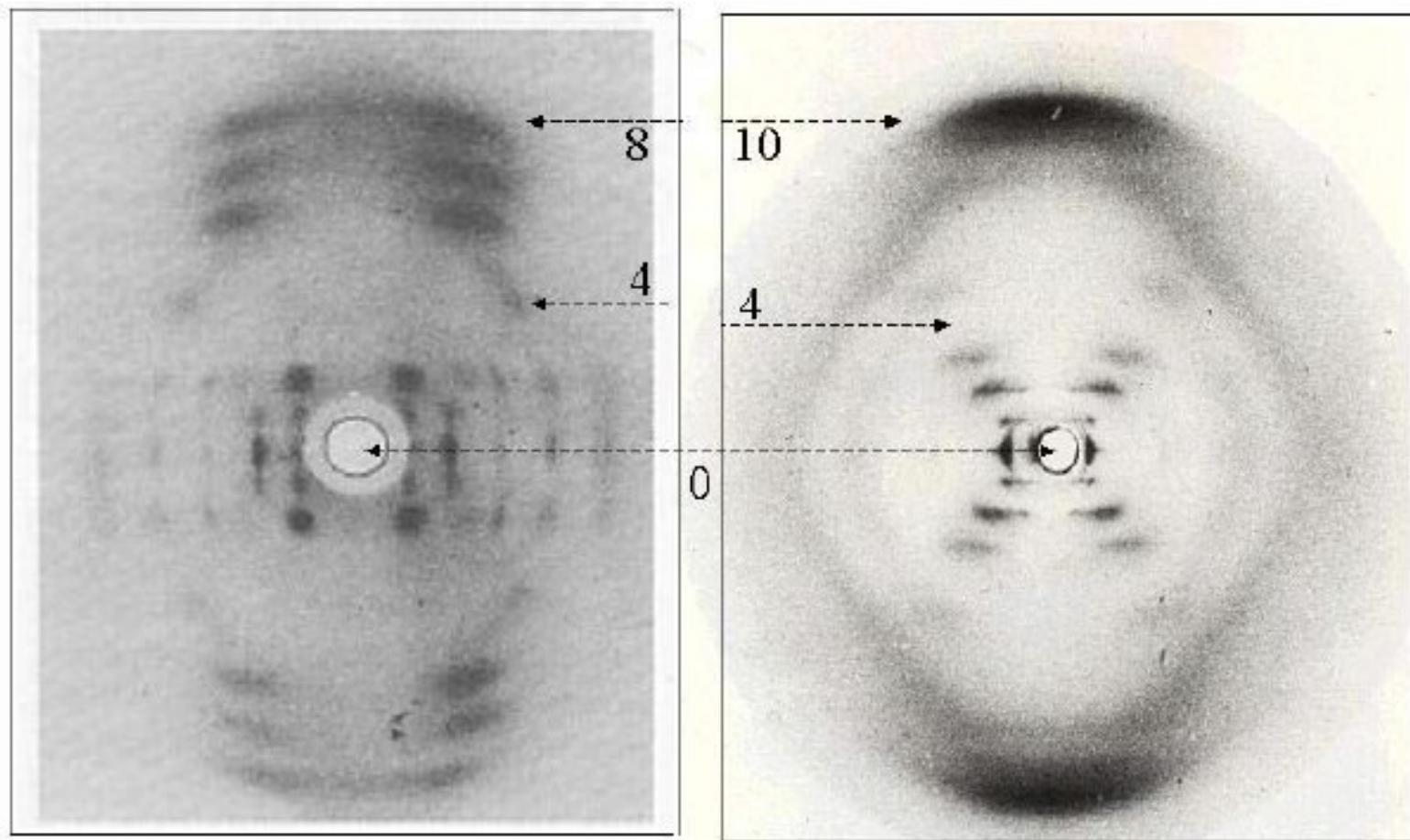


Fig. 3

Fig.3 Computer simulated pattern of X-ray diffraction by a phosphorus helix of period  $P$ , radius  $r$  and atomic repeat  $p_a$  (see Table I for the leading Bessel contributions). Notice the central St Andrew's cross, the Bessel oscillations along the layer lines and the diamond pattern (highlighted by broken lines) with nearly empty North and South diamonds. The structural parameters of the helix ( $P$ ,  $r$ ,  $p_a$ ) are readable from the geometrical parameters of the pattern ( $2\pi/P$ ,  $\alpha$ ,  $2\pi/p_a$ ).

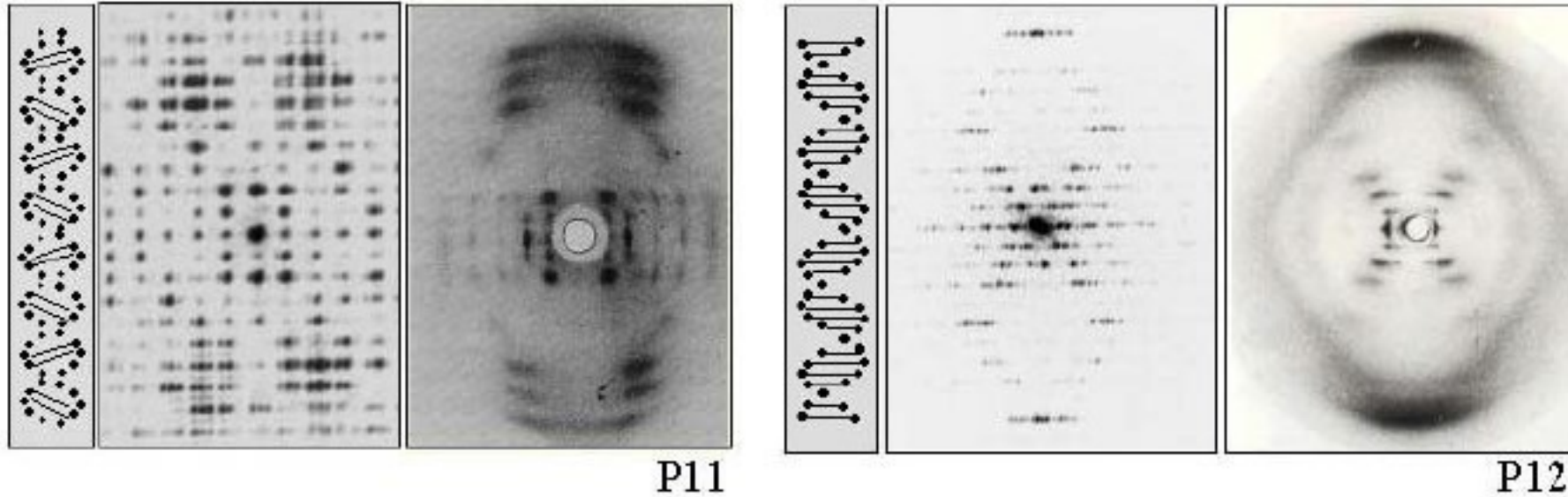


(a) *A-DNA*

(b) *B-DNA*

Fig.4

Fig.4 The historic X-ray fibre diffraction patterns (a) of *A-DNA* and (b) of *B-DNA* plotted on the same scale. The 8<sup>th</sup> layer line of pattern (a) occurs at about the 10<sup>th</sup> layer line of pattern (b) reflecting a 20% increase in the DNA helix period. The *A-DNA* pattern shows crystalline spots on the first few layer lines.



P11. *Optical simulation of the X-ray diffraction by an A-DNA fibre. The motif on the left is arranged on a 2-D lattice in panel P11 of the slide. The strong features on the 6 to 8<sup>th</sup> layer lines of both the X-ray picture and the simulated pattern arise from the inclined base pairs seen edge on and forming a zigzagging double slit grating. (compare with P5).*

P12. *Optical simulation of the X-ray diffraction by a B-DNA fibre. The strong streaks on the 10<sup>th</sup> layer lines of both the X-ray picture and the simulated pattern arise from the horizontal base pairs seen edge on.*